

Heat wave tracker: A multi-method, multi-source heat wave measurement toolkit based on Google Earth Engine

Mingxi Zhang^{a,b,c}, Xihua Yang^{a,c}, Jamie Cleverly^{a,d}, Alfredo Huete^a, Hong Zhang^a, Qiang Yu^{e,*}

^a School of Life Sciences, Faculty of Science, University of Technology Sydney, PO Box 123, Broadway, NSW, 2007, Australia

^b Soil and Landscape Science, School of Molecular and Life Sciences, Curtin University, GPO Box U1987, Perth WA, 6845, Australia

^c NSW Department of Planning, Industry and Environment, 4 Parramatta Square, Parramatta, NSW, 2150, Australia

^d Terrestrial Ecosystem Research Network (TERN), College of Science and Engineering, James Cook University, Cairns, Qld, Australia

^e State Key Laboratory of Soil Erosion and Dryland Farming on the Loess Plateau, Northwest A&F University, Yangling, 712100, Shaanxi, China

ARTICLE INFO

Keywords:

Extreme heat wave
Google Earth Engine
Climate datasets
Risk analysis
GCM
Australia

ABSTRACT

Under ongoing global warming due to climate change, heat waves in Australia are expected to become more frequent and severe. Extreme heat waves have devastating impacts on both terrestrial and marine ecosystems. A multi-characteristic heat wave framework is used to estimate historical and future projected heat waves across Australia. A Google Earth Engine-based toolkit named *heat wave tracker* (HWT) is developed, which can be used for dynamic visualization, extraction, and processing of complex heat wave events. The toolkit exploits the public long-term high-resolution climate datasets to developed nine heat wave datasets across Australia for extreme heat wave value analysis. To examine climate change on heat waves and how they vary in time and space, we also explore the probability and return periods of extreme heat waves over a period of 100 years. The datasets, toolkit and findings we developed contribute to global studies on heat waves under accelerated global warming.

1. Introduction

Under ongoing global warming due to climate change, heat waves are expected to become more frequent and severe in the future (IPCC, 2019). Extreme heat waves during the last two decades have been recorded across many regions in the world such as those in Europe in 2003 (Schär et al., 2004), Moscow region in Russia in 2010 (Rahmstorf and Coumou, 2011), and Australia in 2013 (Lewis and Karoly, 2013). Heat waves in Australia incur significant hazard for both humans and ecosystems and cause more deaths than other natural hazards including floods, storms and bushfires. In terms of heat wave impacts on ecosystems, extreme heat waves increase the probability of bushfire risk, affect crops and food security for terrestrial systems (Luo, 2011), and cause catastrophic damage to marine ecosystems (Hobday et al., 2016). Moreover, extreme temperatures contribute to widespread unfavorable health outcomes and even the death of vulnerable people.

Although heat wave is commonly known as a period of exceptional hot weather event, there is currently no universal informative measurement in climate science community (Alexander and Perkins, 2013). To overcome these issues, a set of climate indices developed by the

Expert Team on Climate Change Detection and Indices (ETCCDI) have been widely applied to observational and modeled climate data to understand previous and future changes in extreme heat wave events (Zhang and Yang, 2004; Alexander et al., 2006). The work by ETCCDI is extensively recognized as pioneering, however, the indices only measure one feature of extreme events such as frequency, intensity or duration (PERKINS, 2015). A comprehensive and consistent analysis of heat waves is required, which should consider multi-characteristics of heat wave events, namely: i) frequency, ii) intensity, iii) duration, and iv) spatial extent (Raei et al., 2018). The multi-characteristic heat wave definition method used in this study is from a well-known heat wave framework constructed by Alexander and Perkins (2013) and includes: a minimum temperature approach, a maximum temperature approach, and an excess heat factor (EHF) approach. This framework has proven to be successful in measuring historical and future projected heat waves.

However, useful public software or tools that identify all the required characteristics of heat waves (frequency-intensity-duration-spatial extent) are still rare. Most studies with their own tools cannot fully reflect the four characteristics of complex heat wave events (Feron et al., 2019; Lyon et al., 2019; Li, 2020). By summarizing the classical heat

* Corresponding author. State Key Laboratory of Soil Erosion and Dryland Farming on the Loess Plateau, Northwest A & F University, Yangling 712100, China.
E-mail address: yuq@nwfau.edu.cn (Q. Yu).

wave definition, an R package called *heatwaveR* was developed, which provides a comprehensive analysis to detect and visualize ocean heat waves (Schlegel and Smit, 2017). However, it is inefficient when applied to large gridded data products. Global Heat Wave and Warm-spell Data Record and Analysis Toolbox (GHWR) which is a MATLAB Toolbox allows processing and extracting heat wave records for any location efficiently. It not only contains multiple definitions but also detects the required multi-characteristics (Raei et al., 2018). However, desktop applications like GHWR still have a bottleneck when encountering the challenges related to accessibility of long-term gridded climate data, data storage and computational requirements. In the current era of big spatial and Earth Observation (EO) data, users need to deal with a vast amount of different spectral, temporal and spatial resolutions data (Gomes et al., 2020). To meet these demands, there is need for novel technologies based on cloud computing to properly extract heat wave information in the server side without having to download vast amounts of climate data and provide dynamic visualization, extraction and processing of complex heat wave events. Google Earth Engine (GEE), a powerful cloud computing geospatial analysis platform, has given researchers the opportunity to use big data for petabyte-scale environmental data analysis (Gorelick et al., 2017).

With the gridded global reanalysed datasets (e.g., Hadley Centre/Global Historical Climatology Network (HadGHCND), Climate Prediction Centre (CPC)) and regional reanalysis datasets (e.g., The COordinated Regional Downscaling EXperiment (CORDEX), Australian Water Availability Project (AWAP)) being freely available, many studies have investigated heat waves at various scales (Perkins et al., 2012; Ma et al., 2020; Christidis et al., 2014). The atmospheric reanalysis datasets are quite useful for gaining understanding in how the heat wave will change. Reanalysis datasets are created by data assimilation and numeric models to represent a synthesized estimate of the atmospheric state and provide global scale dataset over several decades or longer. One benefit of using reanalysis data is that it extends the study to locations without observation records. Another important advantage is that the spatially contiguous heat wave regions derived from the reanalysis data have crucial implications for heat-related impacts such as exposure of the community to extreme heat wave events and high energy demands (Lyon et al., 2019; Li, 2020). However, some heat wave assessments are mostly based on climate datasets with relatively coarse resolution which would affect the representation of heat waves, resulting in biased conclusions. Furthermore, key processes that occur on regional scales may not be adequately simulated. Benefiting from those newly reanalysed climate datasets and high spatio-temporal gridded regional climate datasets, our analysis will explore how these climate datasets differ in representing heat waves and how the methods differ in identifying and characterizing heat waves.

Increasingly, researchers are becoming less interested in data in the “normal” range and more concerned with the ‘abnormal’ and extreme events that are recurrent and unpredictable. Extreme value theory (EVT) is the statistical framework that estimates the probability of an extreme event occurring in the future (Coles et al., 2001). Because of its importance, many public packages and toolboxes over the last decade have been developed to implement various methods from EVT (Ribatet et al., 2011; Cheng et al., 2014; Gilleland and Katz, 2016; Heffernan et al., 2016). It is clear from much of the literature using gridded observed data and projected climate model data at regional and global scales that the probability of extreme heat waves will change over time (Alexander and Perkins, 2013; Purich et al., 2014). Recently, several studies of the risks of heat wave by means of the EVT have been published (Ma et al., 2020; Tanarhte et al., 2015; Shen et al., 2016). However, the precise probabilities of intensity, frequency and duration of extreme heat wave at a continent scale like Australia over the time are still unknown. Meanwhile, the potential impact of climate change on heat wave varies in space and time. In this context, we explore the risk of heat waves in Australia by performing non-stationary analysis of extreme heat waves for the past 100 years.

In this study, we will develop a multi-method global heat wave data record and analysis toolbox (namely *heat wave tracker*) to process and extract heat wave records from multi-source climate datasets. With our toolbox’s computational power in handling long-term high-resolution climate datasets, we developed nine extreme heat wave datasets in Australia for extreme heat wave value analysis. In addition, we first use non-stationary generalized extreme values method to analysis the characteristics of extreme heat wave events in Australia over the past 100 years to help adjust policies for climate change adaptation. Finally, we also explore how the characteristics of heat waves are projected to change across Australia under future climates.

2. Data and methods

2.1. Earth observation datasets

SILO is a database of Australian climate data from 1889 to the present hosted by the Queensland Department of Environment and Science (DES). It provides daily climate variables on a 0.05° grid across Australia for research, modelling and climate applications. The datasets are constructed from observational data obtained from the Australian Bureau of Meteorology (BoM). SILO uses a thin plate smoothing spline to interpolate daily climate variables. There is some evidence that the data quality of maximum and minimum temperatures corresponds strongly to station density, with the largest errors tending to occur where the network of observed stations is sparse (Jones et al., 2009). Currently, SILO data are uploaded into the GEE data catalog and maintained by Earth Observation Data Science (Earth Observation Data Science).

In addition to using high-resolution interpolated climate data, there have been many studies using reanalysed temperature data for heat wave studies, such as the latest fifth generation ECMWF (European Centre for Medium-Range Weather Forecasts) reanalysed climate data (ERA5) and CPC Global Daily Temperature dataset dating back to 1979 (Physical Sciences Laboratory). ERA5 combines physical modeling and data assimilation into a complete hourly-based and consistent dataset. For example, minimum and maximum daily air temperature at 2 m from ERA5 Daily are calculated based on the hourly 2 m air temperature data. The ERA5 Daily used in this study were obtained within the GEE Data Catalog (Copernicus Climate Change Service). CPC Global Daily Temperature dataset includes both daily T_{max} and T_{min} on a 0.5×0.5 grid from 1979 to the present. This product is constructed by a combination of two weather station datasets around the world, namely Climate Anomaly Monitoring System (CAMS) and Global Historical Climatology Network version 2 (GCHN). These two datasets together have about 10978 stations around the global, the temperatures from which are gridded using Inverse Distance Weighting (IDW) interpolation algorithm. In addition, the temperature lapse rate estimated from observation-based global reanalysis temperatures are used to make topographical adjustments. Note that observations from CAMS and GCHN have less coverage over central Australia and good coverage over USA, Europe and China. The lack of accuracy from the sparse density of observation stations would impact the identification of heat wave events. In this study, CPC dataset netCDF4 files have been transformed into GeoTIFFs format using R scripts and uploaded into the GEE Catalogue for further analysis.

For projection periods (2006–2100), Coupled Model Intercomparison Project Phase 5 (CMIP5) that have daily maximum and minimum temperature from the historical experiment and two representative concentration pathway (RCP) experiments (RCP4.5 and RCP8.5) are analyzed in this study. Within the GEE data catalog, the NASA NEX dataset contains daily downscaled projections of 21 GCMs under the CMIP5 across two greenhouse gas emissions scenarios (Thrasher et al., 2012). CMIP5 reference periods (1975–2005) and projection periods (2006–2100) which contain daily maximum and minimum temperature are used to construct multi-model mean composites for summer heat wave under two RCP emission scenarios.

2.2. Heat wave indices

The core algorithms behind the toolbox are based on a general heat wave framework which employs three separate heat wave identification methods (daily minimum and maximum temperature, and the excess heat factor) and use the fixed and dynamic thresholds as the baseline to determine a heat wave event which has at least three days in a row where the threshold is exceeded. From a climatological perspective, heat wave indices with absolute thresholds such as ETCCDI may only be suitable when studying heat waves in a small region where a single climate regime exists. However, for large regional or continental studies like Australia where a broad range of climates exist, three separate heat wave identification methods used in this study can be readily calculated from climatological data is more applicable for representing heat wave occurrence across multiple climates. Of which, EHF is not only more sensitive than other heat wave indices in measuring heat waves, but is also the official definition used Australia-wide (Alexander and Perkins, 2013; Nairn and Fawcett, 2015). For each grid point, three heat wave indices were calculated for the Australian warm season from November to March. These indices include:

- 1) TX90pct—The 90th percentile of Tmax in calendar day based on a centered 15-day window (i.e., 7 days after and before a calendar day). The thresholds are calculated for each time period and grid point separately.
- 2) TN90pct—The 90th percentile of Tmin in calendar day, same time period and unit as Tmax.
- 3) Excess heat factor (EHF) – EHF is a product of two metrics based on Tmean: EHI_{sig} and EHI_{accl} ; The first index is denoted as ‘significance’ (EHI_{sig}) and determines how extreme the temperature conditions are by comparing the previous 3-day mean with climatology (the 95th percentile of the daily mean temperature calculated over the period of reference) (Equation (1)); The second index is a measure of acclimatization (EHI_{accl}) and the difference of the 3-day mean to the previous 30-day mean (Equation (2)). With this second index, heat stress is only likely to occur in summer. From Fig. 1, the threshold 0 means the unusual 3-day mean temperature is above the 95th percentile of the average temperature over a fixed climatological period. EHF can also be defined as $EHF = |EHI_{accl}| \times EHI_{sig}$, which means EHI_{accl} acts as an amplification term on EHI_{sig} , thus EHF can be negative.

$$EHI_{sig} = (T_i + T_{i-1} + T_{i-2}) / 3 - T_{95} \quad (1)$$

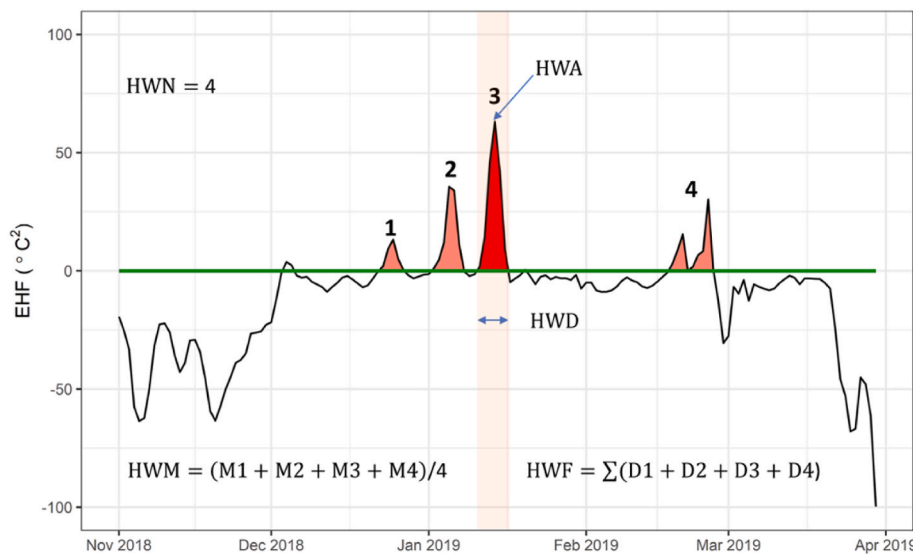


Fig. 1. An example schematic of indices used to define heat wave-EHF. Short duration heat spikes less than three days in a row are not heat waves. In this figure the green line is the threshold and black line is the EHF. There are four discrete events including red and pink heat spikes (HWN); the highest red heat spikes is the heat wave amplitude (HWA); the length of the longest event is also the red heat spikes (HWD); the average heat wave magnitude is the average magnitude across four events (HWM); and the sum of four heat wave events that above the threshold is HWF. The five indices in the figure are calculated for each season and annually.

$$EHI_{accl} = (T_i + T_{i-1} + T_{i-2}) / 3 - [(T_{i-3} + \dots + T_{i-32}) / 3] \quad (2)$$

$$EHF = EHI_{sig} \times \max [1, EHI_{accl}] \quad \text{Eq (3)}$$

For heat wave identification method based on daily mean temperature, heat wave represented as excess heat factor (EHF) is a product of two metrics: EHI_{sig} and EHI_{accl} . So, the unit of heat wave is given in $^{\circ}C^2$. However, for heat wave identification method based on daily minimum and maximum temperature, heat wave is defined as a spell of at least three consecutive days with daily minimum and maximum temperature exceeding the local 90th percentile of a centered 15-day of window. Therefore, the unit of heat wave is given in $^{\circ}C$.

Further to these three indices, we used a multi-aspect framework to represent heat wave characteristics including:

- (1) Heat Wave Number (HWN) - the total number of discrete heat wave events;
- (2) Heat Wave Duration (HWD) - the length of the longest heat wave event;
- (3) Heat Wave Frequency (HWF) - the sum of days satisfying positive heat wave values;
- (4) Heat Wave Amplitude (HWA) – the peak magnitudes (the highest value of the heat wave in a season);
- (5) Heat Wave Magnitude (HWM) – the mean magnitudes (average magnitude across all heat waves);

Among them, HWM and HWA are measures of heat wave intensity, while HWD, HWF and HWN are measures of heat wave longevity.

2.3. Non-stationary generalized extreme value analysis

Extreme value theory has a rigorous framework for analysis of climate extremes and their return levels (Coles et al., 2001). Generalized extreme value (GEV) distribution is a combination of three limiting distributions: Gumbel, Fréchet, or Weibull comes from the limit theorems for block maxima/minima or annual maxima/minima (Katz, 2010). A variety of studies apply the GEV to analyze climatic extremes. This technique is often referred to as the block maxima approach. Another form of the EVT is known as the peak-over-threshold (POT) approach, in which extreme values above a high threshold are analyzed using a generalized Pareto distribution. Both block maxima approach and POT are widely applied in studying climatic extreme events. The cumulative distribution function of the GEV can be expressed as:

$$\psi(x) = \left\{ - \left(1 + \xi \left(\frac{x - \mu}{\sigma} \right)^{\frac{1}{\xi}} \right)^{-\xi}, \left(1 + \xi \left(\frac{x - \mu}{\sigma} \right)^{\frac{1}{\xi}} \right) > 0 \right. \quad (4)$$

The GEV distribution has three distribution parameters $\theta = (\mu, \sigma, \xi)$: (1) the location parameter (μ) determines the center of the distribution; (2) the scale parameter (σ) specifies deviations around μ ; and (3) the shape parameter (ξ) governs the tail behavior of the GEV distribution. For $\xi > 0$ $\xi \rightarrow 0$, and $\xi < 0$ leads to Frechet distributions, Gumbel distribution and Weibull distribution, respectively.

The extreme value theory for stationary random sequences has been extensively studied. In this study, a stationarity process assumes no change to extreme's properties while a non-stationary process is time-dependent, and the properties of the distribution would change in the future. The location parameter is assumed to be a linear function of time to account for non-stationarity, while keeping the other two parameters constant:

$$\mu(t) = \mu_1 t + \mu_0 \quad (5)$$

where t is the time (in years), and $\beta = (\mu_1, \mu_0, \sigma, \xi)$ are the parameters. In this study, a practical package named *Non-stationary Extreme Value Analysis (NEVA)* Matlab package was introduced for assessing extremes in a changing climate. *NEVA* offers a framework for performing non-stationary analysis of extremes and provides non-stationary effective return levels with t -year return period, and risks of climatic extremes using Bayesian inference and also includes simulated ensembles with upper bound and lower bound (Cheng et al., 2014). This study estimated extremes heat wave metrics based on non-stationary Maximum Likelihood Estimators. Here, from the long term (1920–2019) time series of heat wave magnitudes, non-stationary GEV was fitted together with the standard error using R package *Introduction to Statistical Modeling of Extreme Values (ismev)*. We kept the scale and shape parameters constant, while the location parameters were calculated from the regression parameters (μ_1, μ_0) of Equation (5) at the median of the corresponding time period. For example, the median of the corresponding time was 1970 over the period 1920–2019. For the sub-time periods (1980–2019), the estimation for the non-stationary GEV distribution is similar.

2.4. Online heat wave measurement under a framework

The heat wave tracker is to facilitate the exploitation of the up-to-date climate data described in Table 1 by providing users a multi-characteristic and multi-source heat wave measurement toolkit. The entire process of heat wave measurement at a continental scale is shown in Fig. 2. The required inputs for our online system include the historical climate data and their future projection. With long time series of climate data, two separate methods were used to calculate fixed and dynamic thresholds. The fixed thresholds are calculated by the 95th percentile of a fix reference period. The dynamic thresholds are based on the 90th percentile of a temporal moving window. Three separate heat wave indices were then used to determine the heat wave characteristics. The core algorithm contains five iterations, three band math operations and two spatial operations to retrieve five heat wave characteristics at each

Table 1
Datasets used in this study.

Dataset Name	Spatial Resolution	Time Period	Data Source
SILO	0.05 × 0.05	1920–2020, daily	EO Data Science (GEE)
ERA5	0.25 × 0.25	1979–2020, daily	ECMWF reanalysis climate data (GEE)
CPC	0.5 × 0.5	1979–2020, daily	CPC global temperature (NOAA)
CMIP5	0.25 × 0.25	1950–2099, daily	NASA NEX-GDDP (GEE)

grid. The first iteration is to do an accumulation of the number of positive values of heat wave indices. The second and third iteration are combined to detect heat wave events, defined as a spell of at least three consecutive days with values of heat wave indices exceeding the threshold. The fourth iteration is used to find the end point of each heat wave events. The fifth iteration is used to accumulate the positive values of heat wave indices. Based on those extreme value analyses and heat wave characteristics database, we created an online heat wave tracker app for public users.

3. Results

3.1. Heat wave tracker

Heat wave tracker is a user-friendly web tool we developed in Google Earth Engine (GEE). The temperature datasets and heat wave definition outlined above are integrated into this online software tool to study heat waves in Australia. The first step is to pre-define the temperature above a certain threshold and pre-process the corresponding five-month long heat wave records. More precisely, thresholds from the reference period of SILO data (1960–1990) and the reference of ERA5 data (1979–1999) were calculated beforehand. Then, the multi-source heat wave record datasets (e.g., heat wave records between 1990 and 2019 are from SILO, 2000–2019 are from ERA5, 2000–2019 are from CPC, 2030–2099 are from CIMP5) using multi-method are generated and stored in GEE cloud data catalog for further visualization analysis to decrease processing times. Subsequent steps are performed in the graphical user interface (GUI), the users can define the point of interest and select the year, data type, heat wave identification method and run the program. Then the tool will plot several figures displaying the time-series of heat wave records and five heat wave metrics maps (HWN, HWD, HWF, HWM, HWA). The information can also be exported (e.g., CSV files) for further analysis. In such a case, analysis-ready heat wave records prove to be a practical and economical way for real-time and human-interactive visualization. Heat wave tracker is freely available from the authors for educational and academic purposes at <https://github.com/geogismx/Heatwavetracker>. The online tool is publicly available at <https://tensorflow.users.earthengine.app/view/heat-wave-tracker>. While we have focused on the heat waves of Australia, users can also define their own research area and produce their heat wave outcomes. For example, users can even use the tool to evaluate the global heat wave with ERA5 datasets.

3.2. How do the datasets differ in representing heat waves?

Despite the use of the same heat wave definition (EHF), different temperature datasets may provide different heat wave metric maps. It relates to the issues of spatial resolution, instrumentation, and data quality. An example of the spatial variation from different climate datasets for heat wave metrics identification is given in Fig. 3, which shows the heat waves across Australia in 2018–2019 (over the period of November–December–January–February–March) from SILO gridded datasets, ERA5 reanalysis datasets and CPC Australia daily temperature datasets. Generally, climate datasets with a high spatial resolution are much smoother than those with lower spatial resolution (seen in Fig. 3).

Each heat wave metric between the three datasets shows similar data range on the color scale. However, the contiguous spatial distribution clearly differs between the three datasets. Specifically, the extreme HWA for each dataset all occur over southern Australia while northern Australia does not experience extreme heat waves. HWA can increase up to 80°C² in the northwest of NSW. In ERA5, larger HWA values are more confined to lower elevations of southern Australia, whilst HWA in SILO and CPC also appear in the central areas. Similar to HWA, the spatial pattern of HWM is mainly centered around the south coast and north-west of NSW. However, the anomalous red spots of HWM in CPC may be caused by the coarse resolution. It is interesting to note that the HWF

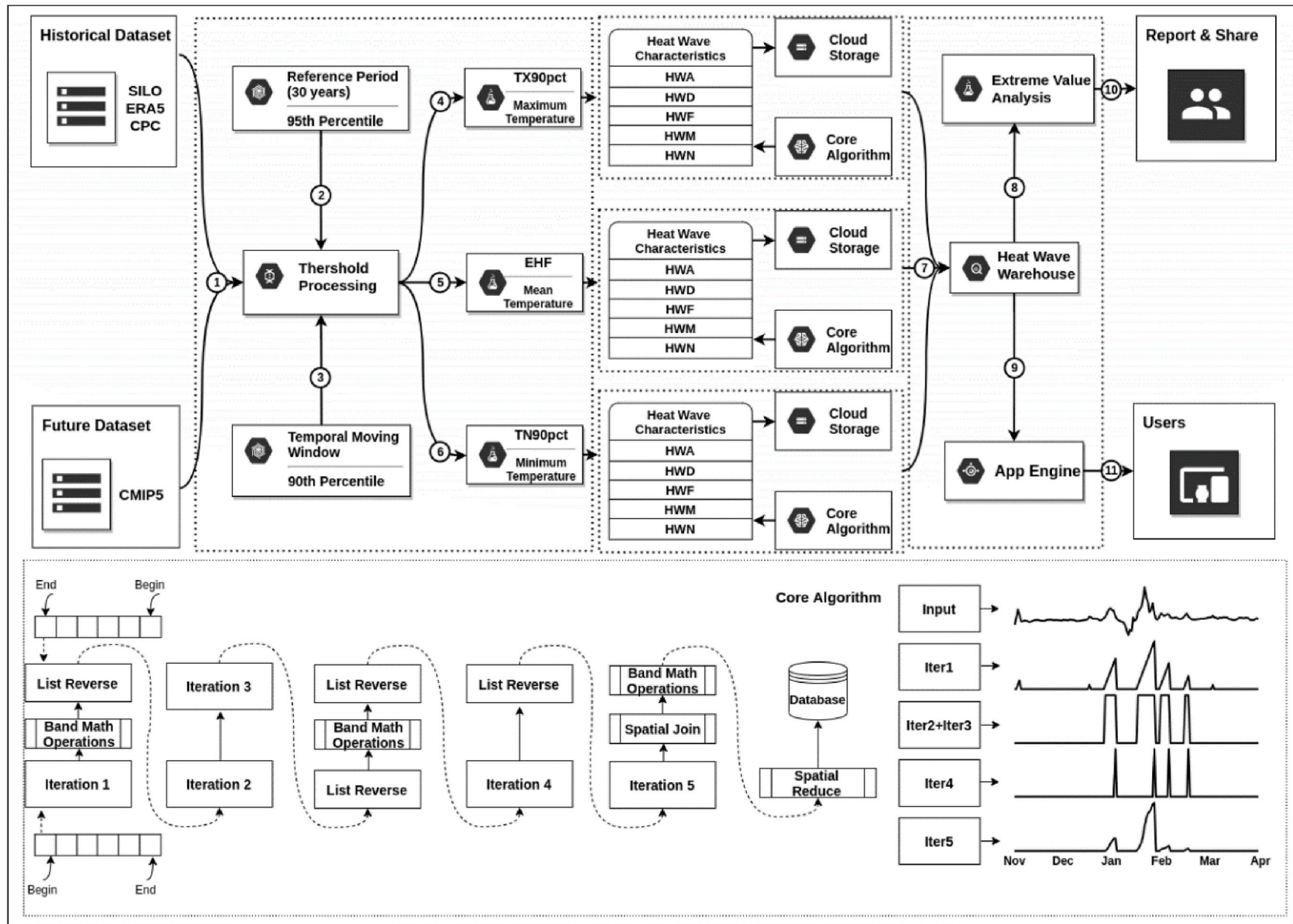


Fig. 2. The online implementation of heat wave tracker toolkit based on Google Earth Engine, using a framework enables climate data integration for heat wave measurement at a continental scale.

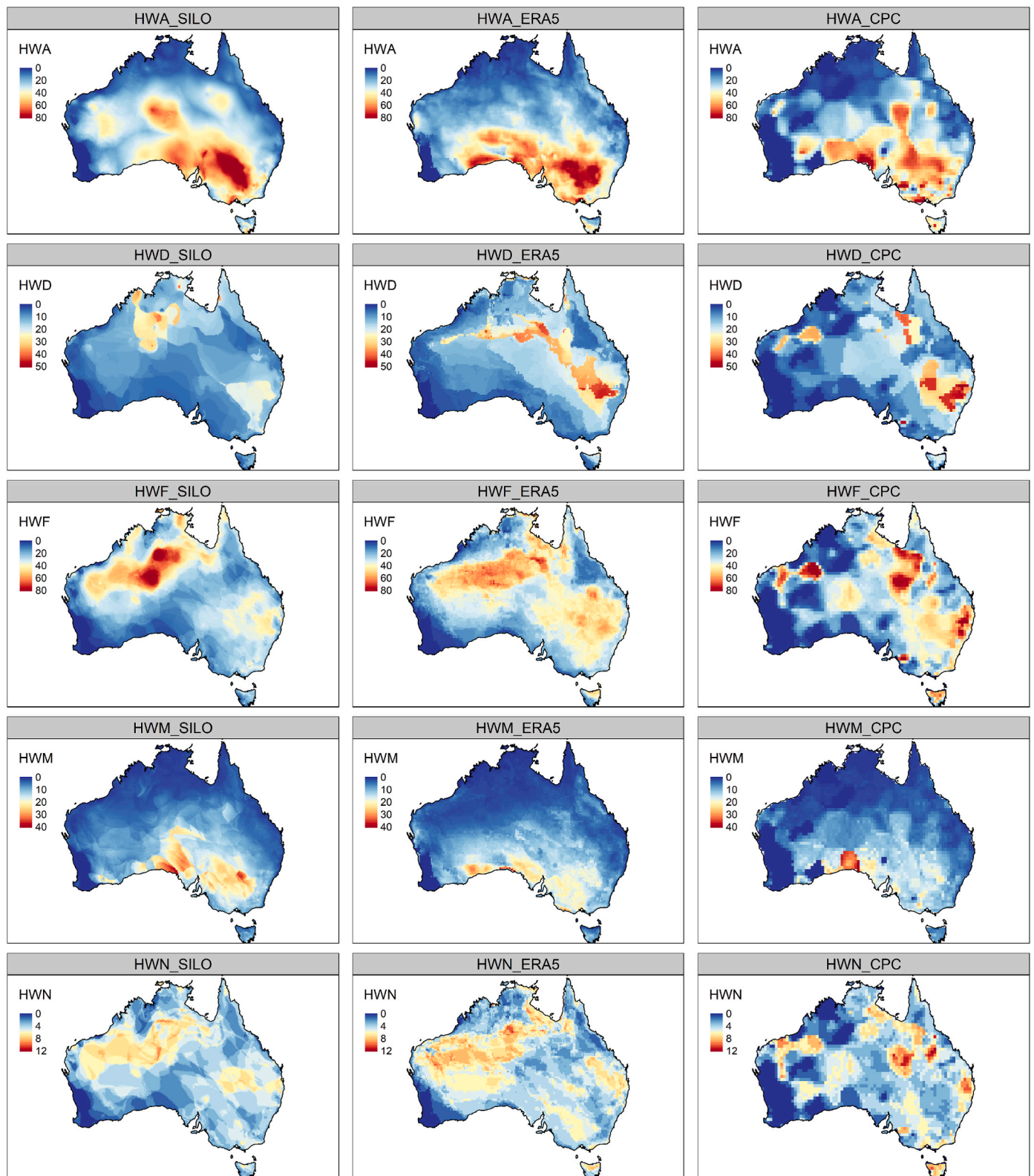


Fig. 3. Examples of heat wave aspects derived from three different climate datasets in 2018.

and the HWN are similar but do not always overlap. From these three datasets, we can see that the HWF and HWN are located in north western and southeast Australia. We also find that HWN from CPC can reach up to 12 times per year and is about two times larger than that from SILO and ERA5, implying that caution should exert when using CPC. The HWF has some influences on HWD, which means the extent of HWD

almost falls in the regions of HWF.

Since local scale differences can not be detected by simple visualization or in cell by cell comparison, we used a map comparison method named the structural similarity index (SSIM) to identify local differences in terms of mean, variance and covariance between two maps (Jones et al., 2016; Wiederholt et al., 2019; Islam et al., 2020). Based on the

global average value of the SSI metric, we try to provide a quantitative analysis of which climate data set is more reliable with respect to five aspects—HWA, HWD, HWF, HWM, HWN. From Table 2, we can see that the similarities between three gridded datasets in terms of five aspects are quite different. There is strong similarity between ERA5 and SILO (0.78) in HWA. The SSI between CPC and ERA5 in HWA is similar (0.68) but weaker for SILO (0.67). The strong level of SSI between ERA5 and SILO (0.77) is also found in HWD, while ERA5 and CPC has a similarity of 0.67, the weakest similarity of 0.66 is from SILO and CPC. The occurrence-based aspects like HWF and HWD lead to reduced similarity. The weaker similarity in HWN exists between three climate datasets, but the SSI between CPC and ERA5 is better (0.56) than CPC and SILO (0.55). Overall, it suggests that ERA5 is the most reliable climate dataset.

3.3. How do the methods differ in identifying and characterising heat waves?

Five heat wave metrics for each method here are defined by ERA5 (seen in Fig. 4). HWA measured by EHF ($^{\circ}\text{C}^2$) tends to be higher than HWA (Tmax, $^{\circ}\text{C}$) and HWA (Tmin, $^{\circ}\text{C}$) due to the different units. Regions that display the higher values in HWA (Tmax) and HWA (Tmin) are very similar, mostly located in the southeast and central Australia. While the EHF-based HWA not only shows higher values in the southeast but also along the coastal regions of South Australia and Victoria. The extreme HWA by EHF all exists in the southward of 20°S . In contrast, HWA is not as large as expected in the northern tropical area. As HWM and HWA are related to heat wave intensity, their spatial patterns are largely similar. For those heat wave aspects (HWD, HWF) related to longevity in different ways, HWD and HWF defined by Tmax and Tmin are similar in spatial structure, which are centered in northwestern Australia and in eastern Australia. However, the lengths of HWD and HWF from Tmax and Tmin are about two times higher than HWD and HWF from EHF. Compared to northwestern Australia, HWF (EHF) is shorter at 60 days. Conversely to HWD and HWF, HWN produces different results in northwestern and eastern Australia where there are larger HWN variations from the EHF method. Fig. 5 shows that the EHF based method identifies four distinct heat wave events, while TX90 based method detects nine heat wave events and TN90 based method finds three heat wave events. The EHF method can combine the characteristics of both TX90 and TN90.

3.4. How does the heat wave risk change in recent climates?

To explore the heat wave risk in recent climates, the average values of HWA (the highest value of the heat wave in a season) over Australia for the past 100 years were used. Non-stationary return levels based on HWA versus the time covariate across the whole continent were generated by NEVA. As shown in Fig. 6a, the effective return levels vary over time indicating return level should be chosen for years to have the same probability of occurrence. For example, the effective return level (HWA) corresponding to a 25-year event during 1920–1944 is 37°C^2 ; the effective return level for a once-in-50-year event (1920–1969) should be 45°C^2 and the effective return level for a 100-year period (1920–2019) is 60°C^2 . In Fig. 6a, we also observe that there is a strong upward trend ($p < 0.005$) for HWA over Australia during the 1920–2019 period. This

Table 2

Structural similarity index between different heat wave characteristics from three climate datasets.

Heat wave characteristics	ERA5_SILO	ERA5_CPC	SILO_CPC
Global SSI _{HWA}	0.78	0.68	0.67
Global SSI _{HWD}	0.77	0.67	0.66
Global SSI _{HWF}	0.71	0.59	0.58
Global SSI _{HWM}	0.76	0.74	0.69
Global SSI _{HWN}	0.59	0.56	0.55

suggests that heat wave amplitude was increasing under climate change. Fig. 6b compares the probability density functions (PDF) of the HWA under two different time intervals (1920–2020, 1980–2020). We find that there is an obvious warming shift of PDFs of the HWA during 1920–2020 compared with that during 1980–2020. This is consistent with the observed increasing trend in Fig. 6a. In addition, the warm tail of the PDFs for the period of 1980–2019 is greater than that of 1920–2019 implying that extreme heat events have much higher probability with effects of climate change. We also find that the 2019 heat wave event is not rare (over 10-year effective return levels, Fig. 6a), with the PDF observed in 2019 for the 1980–2020 higher than that for the 1920–2020 as shown in Fig. 6b. From the long-term (1920–2019) and the short-term (1980–2019) time series of HWA, GEV fits were estimated together with the corresponding ± 1.96 standard error for a 95% confidence interval in Fig. 6c. It denotes that the 2019 heat wave (HWA is 45.6°C^2) has a lower probability of occurrence over 1920–2020 climate and a higher probability over 1980–2020 climate (over 10-year return periods for GEV fit 1980–2020, Fig. 6c).

3.5. How does the heat wave risk change under future climate conditions?

Fig. 7 shows the near-future (2030–2060) and far-future (2069–2099) projected HWA using CMIP5 GCM datasets under two emissions scenarios compared with the 1976–2006 climate. Overall, HWA is projected to increase significantly during the two future periods and a larger fraction of southern Australia is projected to experience more extreme heat wave events. We also see that the average HWA derived from CMIP5 multi-GCM ensemble mean ranges from 0 to 10°C^2 , and HWA decreases equatorward to $\sim 3^{\circ}\text{C}^2$ in the northern Australia. Under the two future periods of RCP4.5, the spatial extent of HWA mainly aggregates in the southern Australia. Compared with HWA in the near-future, HWA in the far-future expands from southeast to western and central Australia. Under the two future periods of RCP8.5, HWA not only increases its intensity but also expands from south to north. As expected, the change in HWA from RCP8.5 is more extreme than that from RCP4.5, indicating that greenhouse warming strongly amplifies the amplitude of heat wave events. Fig. 8 shows the characteristic of HWD changes in the two future periods with different emission scenarios. The patterns of change for HWD are opposite to the change for HWA; northern Australia shows significant increases and southern Australia experience a moderate increase. In the far-future period of RCP4.5, we also note that HWD shows a stronger increase in western coastal areas and in northern tropical Australia, with HWD across northern tropical area reaching ~ 120 days. Again, in the far-future period of RCP8.5, HWD represents an amplification of the RCP4.5 pattern, that is, the duration of heat waves is much stronger than for RCP4.5. This indicates that the duration of southern Australia heat waves is not as sensitive to warming as those in northern Australia, largely due to the southern regions being associated with anticyclones and cold fronts.

4. Discussion

4.1. Model comparison

To evaluate the performance of our model, we made a comparison with GHWR toolbox of Mojtaba Sadegh (2018). For the comparison, the CPC datasets during a period of 1979–2019 were used to model heat wave metrics. Both software toolboxes apply EHF-based method to measure the heat wave metrics. Note that the definition of EHF is composed of the previous three-day mean and the previous thirty-day mean. The threshold of the 95th percentile of Tmean was calculated based on the 20 years period (1979–2009). Two 2018 heat wave indices were obtained from two different software packages. We can see that the spatial pattern of HWD from our model is consistent with that of GHWR (seen in Fig. 9). However, the comparison of HWM shows large difference in spatial patterns. Based on the HWM results of Alexander and

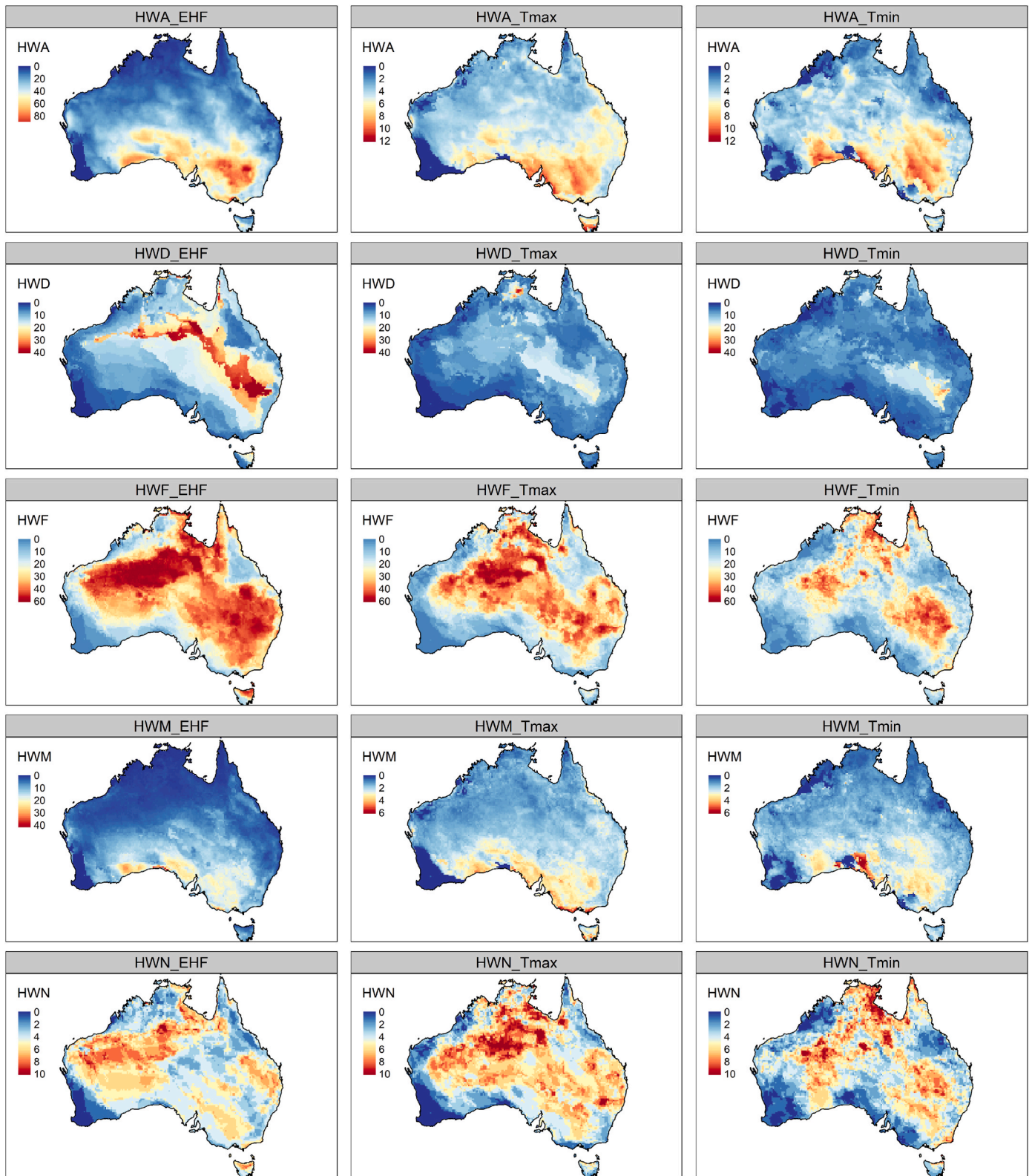


Fig. 4. Examples of heat wave aspects of ERA5 from three different methods in 2018.

Perkins (2013), the HWM of the northern Australia are no more than 12, as the tropical climate imposes less diurnal and seasonal variation in temperature than that in southern Australia. In contrast, the higher HWM values tends to occur in southern Australia and experience higher average peak values. Argüeso et al. (2015) reported higher HWM values towards the south-west of NSW and lower HWM values to the north

coast of NSW, is consistent with the spatial pattern from our model. We also note that the HWM from GHWR (3-day average) has a similar spatial pattern similar to that of HWM from Argüeso et al. (2015), i.e., the highest values of HWM are found in the north-west corner and the lowest values in the mountains of the south. It means that the heat wave metrics from our model are consistent with the original definition of

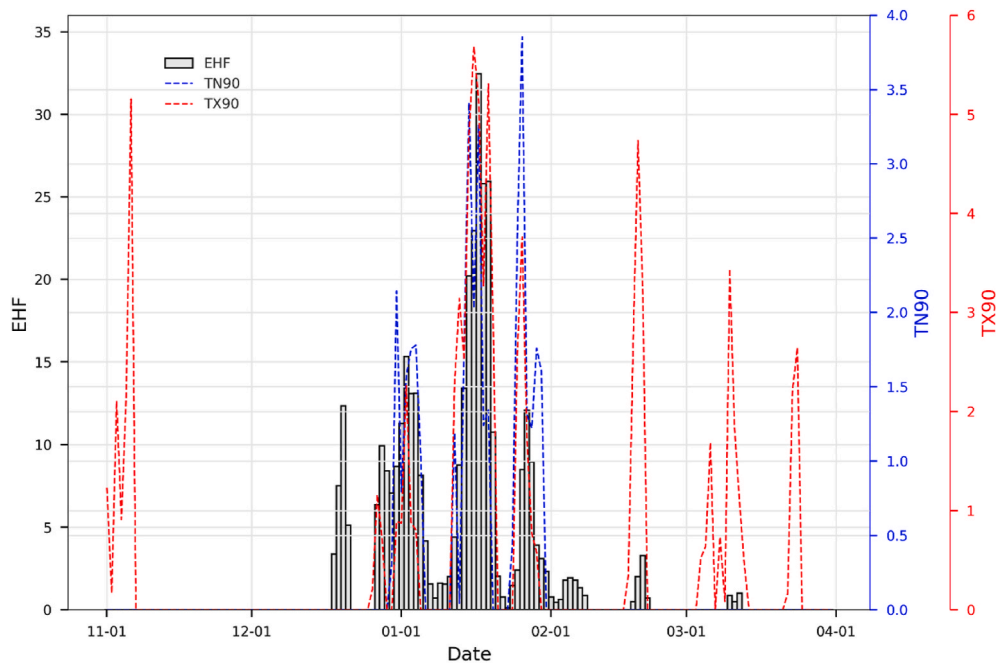


Fig. 5. Distinct heat wave events derived from time series with EHF, TN90 and TX90 at the same point of southeastern Australia.

Alexander and Perkins (2013).

4.2. Heat wave threshold

The CMIP5 multi-GCM ensemble mean projects that longer summer heat waves will occur in northern Australia and hotter heat wave events will increase for southern Australia in the late twenty-first century, with more extreme change in the higher emission scenario RCP8.5 than for the lower emission scenario RCP4.5. The results reveal that the hottest heat waves will increase in southern Australia, which may account for the increasing trend of severe summer bushfires occurring in southeast Australia. Despite the different heat wave definitions and 25-member ensemble mean, our model results are consistent with the results from Purich et al. (2014). However, possibly due to the coarse resolution of the HWD from Purich et al. (2014), trends over Tasmania (an island state) are opposite to the overall pattern of change. While the patterns of change in Tasmania are consistent with the changes in other continental states, it means that our HWD results show promise in simulating fine-scale projections without using downscaling techniques.

Future extreme heat waves in our study are defined relative to a historical reference period, we find a substantial increase in amplitude, duration and extent in both near-future and far-future periods (seen in Figs. 7 and 8). For example, the duration of heat waves can even last over the entire warm season in some areas, which amounts to 152 days. The amplitude of heat waves significantly increases over southern Australia. Such results are not surprising and are in line with other findings (Perkins-Kirkpatrick and Gibson, 2017; Lyon et al., 2019). However, the sensitivity of heat waves to different heat wave thresholds was not explored. Vogel et al. (2020) identified future heat waves with different heat wave thresholds: fixed, seasonally moving and fully moving, where fixed thresholds are based on hot days relative to a historical baseline; seasonal and fully moving thresholds are defined by hot days relative to future conditions. They find that using fixed thresholds might overestimate future heat waves, while using seasonal and fully moving threshold results in little or no changes in future heat wave metrics. To better estimate heat wave characteristics and risk in a warming world, it would be useful to adopt varying heat wave thresholds for future spatiotemporal heat wave studies.

4.3. Future needs

For this study, we use the 5 km SILO gridded climate data, reanalysed data (25 km, 50 km) to estimate the heat wave at a large scale. However, those climate datasets do not take into account the smaller scale temperature variations, that is, the weather stations used to produce the gridded climate data were too sparse to record fine scale variations in extreme temperatures. For example, we find that the gridded climate data have relatively coarse spatial resolutions and cannot meet the need of monitoring heat wave variances in complex settings, and the heat wave maps are generally distributed evenly over urban heat islands. Furthermore, the location of most weather stations is away from building areas and the associated heat islands where extreme heat waves pose the greatest risk to human health. This issue can be at least partially resolved by using satellite thermal infrared sensing method to monitor and analyze heat waves at a local scale.

The proliferation of land surface temperature (LST) products offers an opportunity to study the characteristics of extreme heat waves at the community scale and give insight into urban heat wave planning and the prevention of heat-related mortality. For example, MODIS LSTs have higher spatial resolution (1 km) and temporal resolution (four passes per day). MODIS LSTs provide the maximum and minimum products for the 20 years back to March 5th, 2000, which could be a valuable resource to capture extreme heat waves and for regional and local scale heat wave research. However, it is difficult to map LST accurately as the temperature are very variable and could be affected by climate factors like clouds and wind (Venter et al., 2020).

Compared to daily satellite data from MODIS (four passes a day), Himawari-8 data provides real time data at 10-min intervals, but the spatial resolution is 2 km which is also suitable to conduct regional studies. The high temporal resolution of Himawari-8 can show the diurnal characteristics of extreme heat waves on urban heat waves. Despite the limitations of the relatively short time period (from 2015 to present) of the historical data archive of Himawari-8, a combination of MODIS LST and Himawari-8 LST offers a better solution for obtaining a higher spatial resolution while maintaining a higher temporal resolution, which is extremely useful for characterizing the heat wave characteristics and investigating the relationship between heat waves, land cover and population.

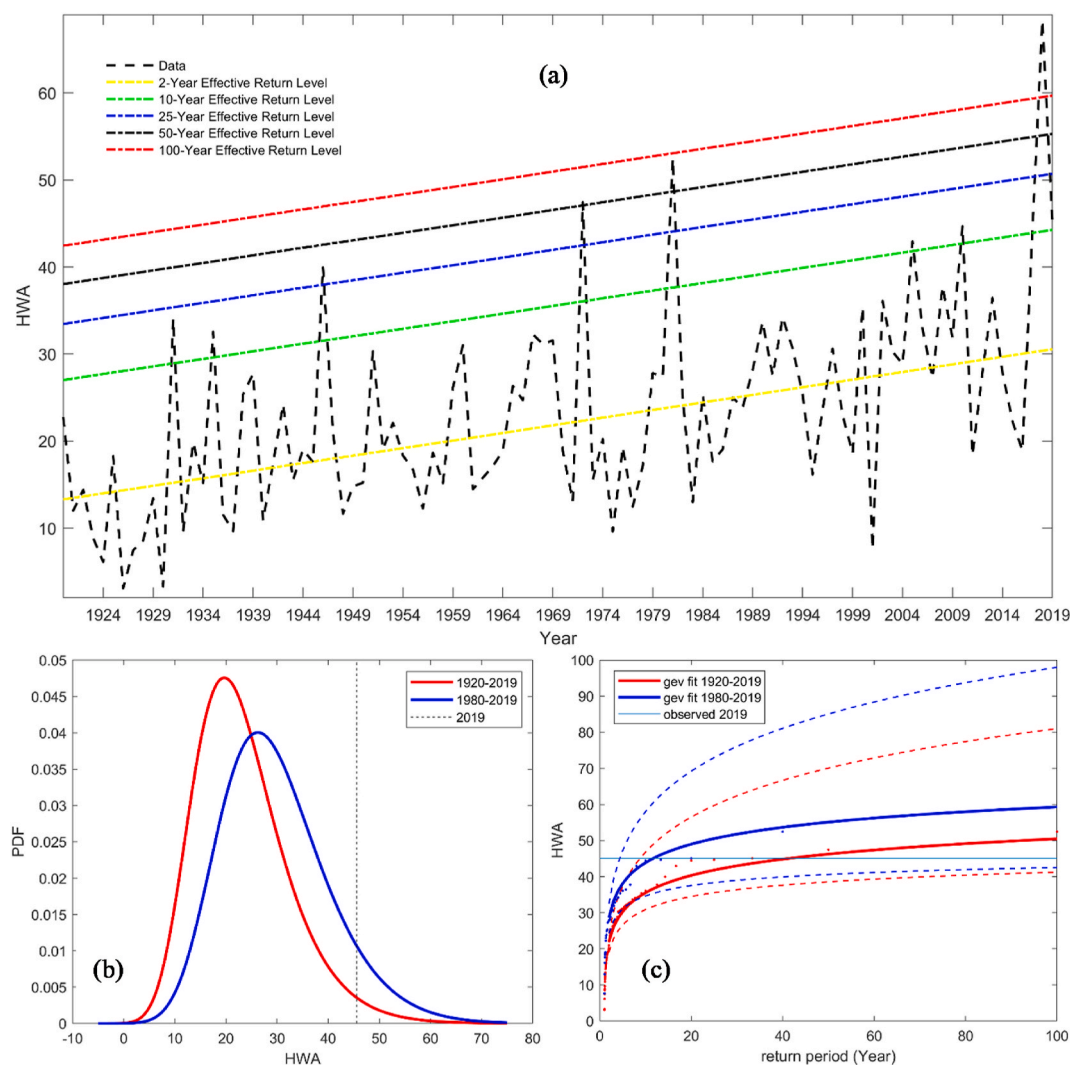


Fig. 6. (a) Effective return level under the non-stationary assumption with mean HWA value from the continental Australia. (b) The probability density functions (PDF) of HWA under 1920–2019 and 1980–2019. (c) Return period of HWA over Australia. The distributions are fit with non-stationary GEV for the climates of 1920–2019 (red), 1980–2019 (blue).

The health or agriculture impacts of heat waves are not only related with temperature measurements, but also affected by some additional factors. For example, health effects are associated with factors including perceived temperature, solar radiation, relative humidity, wind, while for agriculture, the parallel occurrence of droughts is highly relevant. Due to the problems of short time spans, inconsistency, and biases, these additional measurements have limitations on precisely capturing spatio-temporal pattern of heat wave impacts. The reason why we choose temperature-based heat wave definition is because it can be calculated from readily available climatological data and provides information on various aspects of heat waves. In other words, the choice of temperature rather than other measures is based on their feasibility across varying climates on long-term scales. Further, the availability of long-term temperature datasets at finer spatial scales can greatly improve our understanding of heat wave. We concur that the heat wave definitions directly rely on the critical temperature thresholds. However, there is no universal temperature threshold for health impacts because of regional variability of health status, socio-economic factors, and demographic factors (Alexander and Perkins, 2013). This impact also exists in agriculture due to varying regional patterns of plant species and physiology. Therefore, a given threshold suitable in a small region may not be applicable to a continental study like ours. Fischer and Schär (2010) explored health-related heat wave indices in three health factors: heat

wave duration, minimum temperature, and relative humidity. Our study also quantified the heat wave duration, minimum temperature-based heat wave indices. A combined calculation of temperature and humidity will be considered in our future study.

5. Conclusion

We have developed a heat wave toolbox that has the ability to estimate past, current and future changes in heat waves at a continental scale. It uses a well-known heat wave framework constructed by Alexander and Perkins (2013) and considers intensity, frequency, magnitude, duration and areal extent to explore the spatio-temporal evolution of heat wave severity and coverage. This study is the first attempt to estimate heat wave events across Australia using high spatio-temporal climate datasets. With these heat wave aspects from multi-source data and different methods, we were able to investigate the effects of scales, data quality and definition. We find that ERA5 datasets are the best in characterizing the heat wave events. In exploring the role of different methods on the identification of heat waves, we find that heat wave characteristics based on the Excess Heat Factor index integrate the features of both TX90 based and TN90 based methods.

With the past 100 years of heat wave datasets, the HWA average mean values were calculated and used to estimate non-stationary return

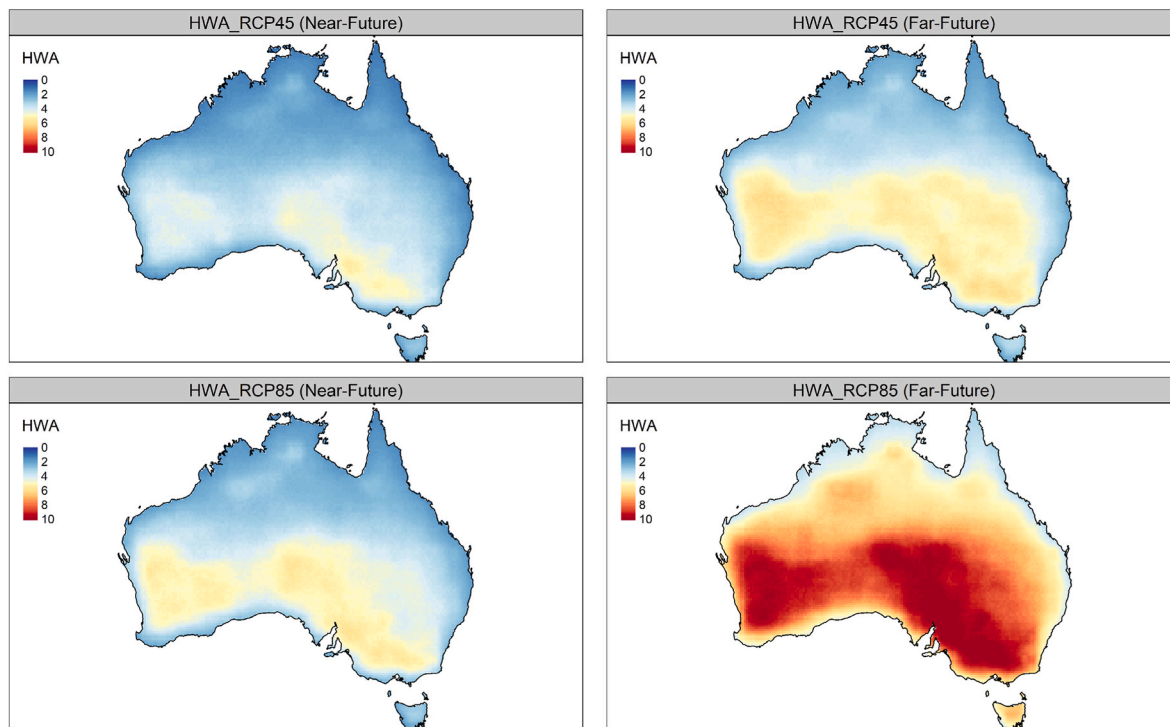


Fig. 7. Near-future (2020–2039) and Far-future (2069–2099) projected climatology for heat wave amplitude obtained from the CMIP5 multi-GCM ensemble.

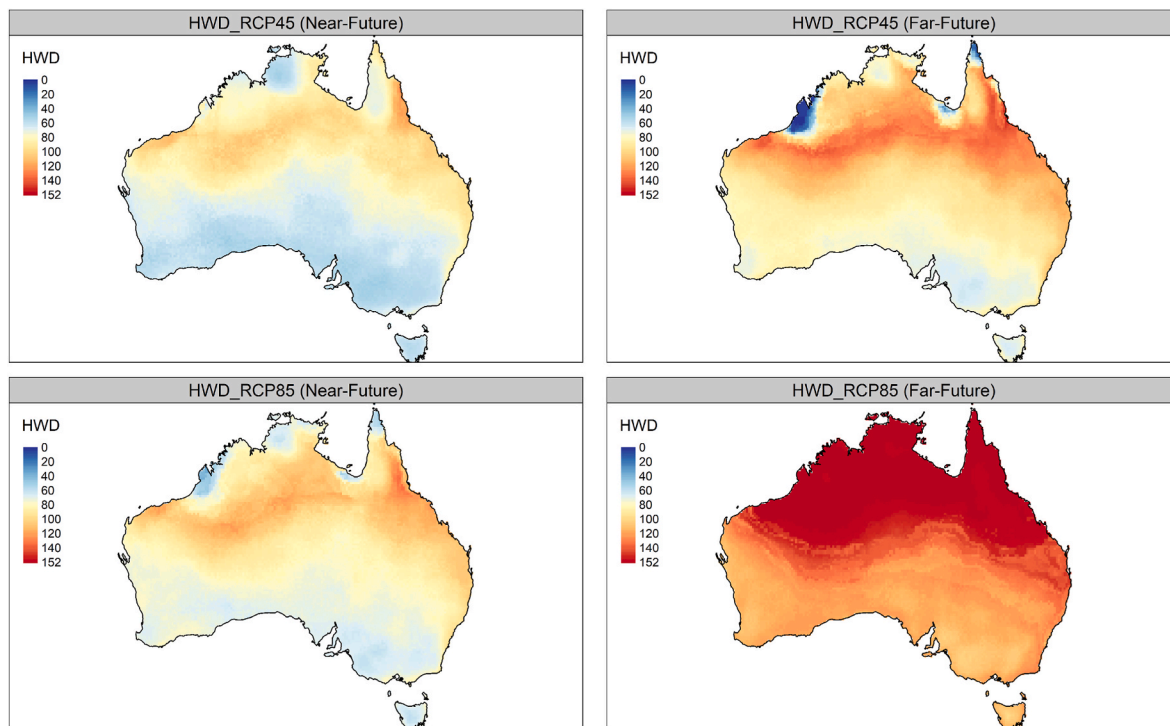


Fig. 8. Near-future (2020–2039) and Far-future (2069–2099) projected climatology for heat wave duration obtained from the CMIP5 multi-GCM ensemble.

levels and return periods. We find that extreme heat wave events have much higher probability due to the effects of climate change. The heat wave event in 2019 may be more frequent in the coming decades. For the climate by the end of century, using heat wave metrics derived from a multi-model ensemble mean, we predict HWA to increase significantly during the two future periods and a larger fraction of southern Australia is projected to experience more extreme heat wave events. Furthermore,

the patterns of change for HWD are opposite to those for HWA; northern Australia shows significant increases and southern Australia experience a moderate increase. The methodology and the cloud computing-based toolbox (HWT) is useful for dynamic visualization, extraction, and processing of complex heat wave events, and applicable anywhere in the world.

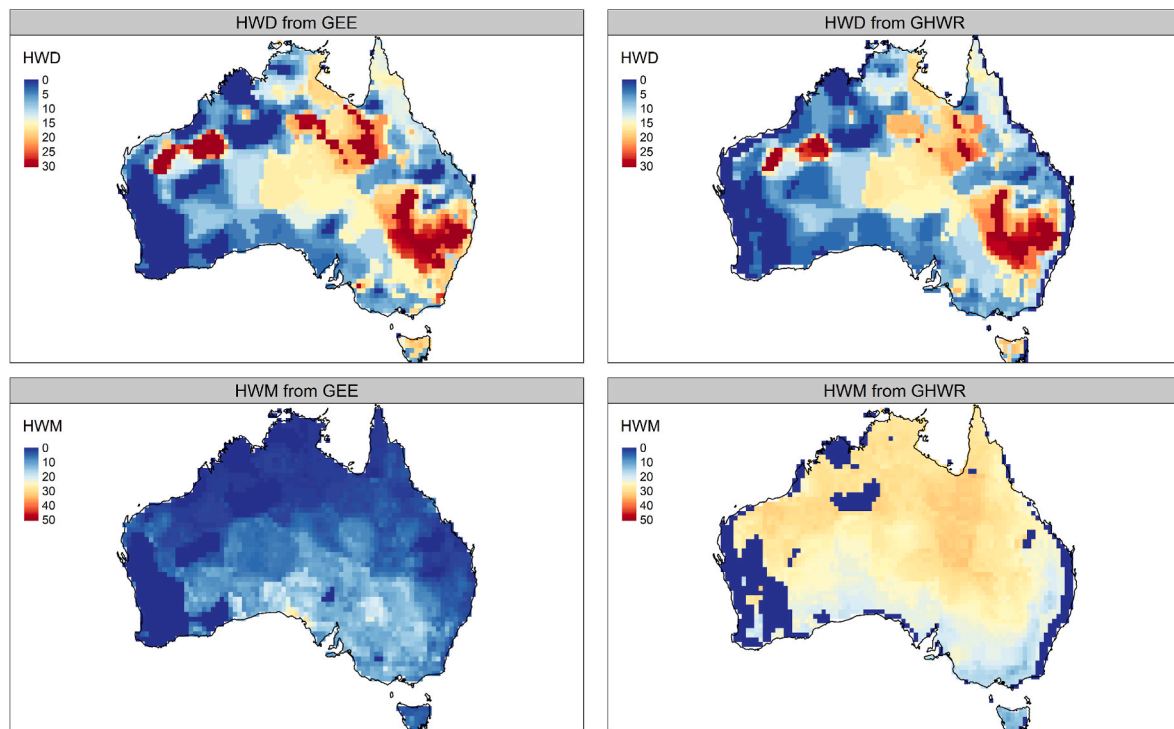


Fig. 9. Heat wave metrics comparison between HWT and GHWR software tools.

Declaration of competing interest

The authors declare that they have no known competing financial interests or personal relationships that could have appeared to influence the work reported in this paper.

Acknowledgements

The first author acknowledges the Chinese Scholarship Council and University of Technology Sydney for scholarships and NSW Department of Planning, Industry and Environment for providing office facilities to conduct this work. The first author also acknowledges Dr Jonathan Gray for article revision help.

References

- Alexander, L.V., Perkins, S.E., 2013. On the measurement of heat waves. *J. Clim.* 26, 4500–4517.
- Alexander, L.V., Zhang, X., Peterson, T.C., Caesar, J., Gleason, B., Klein Tank, A.M.G., Haylock, M., Collins, D., Trewin, B., Rahimzadeh, F., Tagipour, A., Rupa Kumar, K., Revadekar, J., Griffiths, G., Vincent, L., Stephenson, D.B., Burn, J., Aguilar, E., Brunet, M., Taylor, M., New, M., Zhai, P., Rusticucci, M., Vazquez-Aguirre, J.L., 2006. Global observed changes in daily climate extremes of temperature and precipitation. *J. Geophys. Res.* 111.
- Argueso, D.A.D.L., Evans, J., Parry, M., Gross, M., Alexander, L., Green, D., Perkins, S., 2015. Heatwaves Affecting NSW and the ACT: Recent Trends, Future Projections and Associated Impacts on Human Health. NSW Office of Environment and Heritage, Sydney, Australia.
- Cheng, L., Aghakouchak, A., Gilleland, E., Katz, R.W., 2014. Non-stationary extreme value analysis in a changing climate. *Climatic Change* 127, 353–369.
- Christidis, N., Jones, G.S., Stott, P.A., 2014. Dramatically increasing chance of extremely hot summers since the 2003 European heatwave. *Nat. Clim. Change* 5, 46–50.
- Coles, S., Bawa, J., Trenner, L., Dorazio, P., 2001. *An Introduction to Statistical Modeling of Extreme Values*. Springer.
- Copernicus Climate Change Service. ERA5 daily aggregates [Online]. Available: https://developers.google.com/earth-engine/datasets/catalog/ECMWF_ERA5_DAILY. Accessed 2020.
- Earth Observation Data Science. Silo [Online]. Available: <https://www.eodatascience.com/>. Accessed 2020.
- Feron, S., Cordero, R.R., Damiani, A., Llanillo, P.J., Jorquera, J., Sepulveda, E., Asencio, V., Laroze, D., Labbe, F., Carrasco, J., Torres, G., 2019. Observations and projections of heat waves in south America. *Sci. Rep.* 9, 8173.
- Fischer, E.M., Schar, C., 2010. Consistent geographical patterns of changes in high-impact European heatwaves. *Nat. Geosci.* 3, 398–403.
- Gilleland, E., Katz, R.W., 2016. extRemes2.0: an extreme value analysis package in R. *J. Stat. Software* 72.
- Gomes, V.C.F., Queiroz, G.R., Ferreira, K.R., 2020. An overview of platforms for big Earth observation data management and analysis. *Rem. Sens.* 12.
- Gorelick, N., Hancher, M., Dixon, M., Ilyushchenko, S., Thau, D., Moore, R., 2017. Google Earth engine: planetary-scale geospatial analysis for everyone. *Rem. Sens. Environ.* 202, 18–27.
- Heffernan, J.E., Stephenson, A.G., Gilleland, E., 2016. Ismev: an Introduction to Statistical Modeling of Extreme Values. R package version.
- Hobday, A.J., Alexander, L.V., Perkins, S.E., Smale, D.A., Straub, S.C., Oliver, E.C.J., Benthuyzen, J.A., Burrows, M.T., Donat, M.G., Feng, M., Holbrook, N.J., Moore, P.J., Scannell, H.A., Sen Gupta, A., Wernberg, T., 2016. A hierarchical approach to defining marine heatwaves. *Prog. Oceanogr.* 141, 227–238.
- IPCC, 2019. Climate change and land: An IPCC special report on climate change, desertification, land degradation, sustainable land management, food security, and greenhouse gas fluxes in terrestrial ecosystems. In: Masson-Delmotte, V., Shukla, P.R., Skea, J., Calvo Buendia, E., Pörtner, H.O., Roberts, D.C., Zhai, P., Slade, R., Slade, R., Connors, S., Van Diemen, R. (Eds.).
- Islam, M.A., Yu, B., Cartwright, N., 2020. Assessment and comparison of five satellite precipitation products in Australia. *J. Hydrol.* 590.
- Jones, D.A., Wang, W., Fawcett, R., 2009. High-quality spatial climate data-sets for Australia. *Aus. Meteorol. Oceanogr. J.* 58, 233.
- Jones, E.L., Rendell, L., Pirota, E., Long, J.A., 2016. Novel application of a quantitative spatial comparison tool to species distribution data. *Ecol. Indic.* 70, 67–76.
- Katz, R.W., 2010. Statistics of extremes in climate change. *Clim. Change* 100, 71–76.
- Lewis, S.C., Karoly, D.J., 2013. Anthropogenic contributions to Australia's record summer temperatures of 2013. *Geophys. Res. Lett.* 40, 3705–3709.
- Li, X., 2020. Heat wave trends in Southeast Asia during 1979–2018: the impact of humidity. *Sci. Total Environ.* 721, 137664.
- Luo, Q., 2011. Temperature thresholds and crop production: a review. *Climatic Change* 109, 583–598.
- Lyon, B., Barnston, A.G., Coffel, E., Horton, R.M., 2019. Projected increase in the spatial extent of contiguous US summer heat waves and associated attributes. *Environ. Res. Lett.* 14.
- Ma, F., Yuan, X., Jiao, Y., Ji, P., 2020. Unprecedented Europe heat in June–July 2019: risk in the historical and future context. *Geophys. Res. Lett.* 47.
- Nairn, J.R., Fawcett, R.J., 2015. The excess heat factor: a metric for heatwave intensity and its use in classifying heatwave severity. *Int. J. Environ. Res. Publ. Health* 12, 227–253.
- Perkins, S.E., 2015. A review on the scientific understanding of heatwaves—their measurement, driving mechanisms, and changes at the global scale. *Atmos. Res.* 164–165, 242–267.
- Perkins, S.E., Alexander, L.V., Nairn, J.R., 2012. Increasing frequency, intensity and duration of observed global heatwaves and warm spells. *Geophys. Res. Lett.* 39.
- Perkins-Kirkpatrick, S.E., Gibson, P.B., 2017. Changes in regional heatwave characteristics as a function of increasing global temperature. *Sci. Rep.* 7, 12256.

- Physical Science Laboratory. CPC global daily temperature [Online]. Available: <https://psl.noaa.gov/data/gridded/data.cpc.globaltemp.html>. Accessed 2020.
- Purich, A., Cowan, T., Perkins, S., Pezza, A., Boschat, G., Sadler, K., 2014. More frequent, longer, and hotter heat waves for Australia in the twenty-first century. *J. Clim.* 27, 5851–5871.
- Raei, E., Nikoo, M.R., Aghakouchak, A., Mazdiyasi, O., Sadegh, M., 2018. GHWR, a multi-method global heatwave and warm-spell record and toolbox. *Sci. Data* 5, 180206.
- Rahmstorf, S., Coumou, D., 2011. Increase of extreme events in a warming world. *Proc. Natl. Acad. Sci. Unit. States Am.* 108, 17905–17909.
- Ribatet, M., Singleton, R., Team, R.C., 2011. SpatialExtremes: Modelling Spatial Extremes.
- Sadegh, Mojtaba, 2018. Global Heatwave and warm spell toolbox [Online]. Available. https://github.com/mojtabasadegh/Global_Heatwave_and_Warm_Spell_Toolbox, 2020.
- Schar, C., Vidale, P.L., LüTHI, D., Frei, C., HäBERLI, C., Liniger, M.A., Appenzeller, C., 2004. The role of increasing temperature variability in European summer heatwaves. *Nature* 427, 332–336.
- Schlegel, R.W., Smit, A.J., 2017. heatwaveR: a central algorithm for the detection of heatwaves and cold-spells. *J. Open Sour. Software* 3, 1821.
- Shen, L., Mickley, L.J., Gilleland, E., 2016. Impact of increasing heat waves on US ozone episodes in the 2050s: results from a multimodel analysis using extreme value theory. *Geophys. Res. Lett.* 43, 4017–4025.
- Tanarhte, M., Hadjinicolaou, P., Lelieveld, J., 2015. Heat wave characteristics in the eastern Mediterranean and Middle East using extreme value theory. *Clim. Res.* 63, 99–113.
- Thrasher, B., Maurer, E.P., Mckellar, C., Duffy, P.B., 2012. Technical Note: bias correcting climate model simulated daily temperature extremes with quantile mapping. *Hydrol. Earth Syst. Sci.* 16, 3309–3314.
- Venter, Z.S., Brousse, O., Esau, I., Meier, F., 2020. Hyperlocal mapping of urban air temperature using remote sensing and crowdsourced weather data. *Rem. Sens. Environ.* 242, 111791.
- Vogel, M.M., Zscheischler, J., Fischer, E.M., Seneviratne, S., 2020. Development of future heatwaves for different hazard thresholds. *J. Geophys. Res.: Atmosphere* 125.
- Wiederholt, R., Paudel, R., Khare, Y., Davis, S.E., Naja, G.M., ROMÁNACH, S., Pearlstine, L., Van Lent, T., 2019. A multi-indicator spatial similarity approach for evaluating ecological restoration scenarios. *Landscape Ecol.* 34, 2557–2574.
- Zhang, X., Yang, F., 2004. RCLimDex (1.0). *Clim. Res. Branch*.